Variance-based wave function optimization within the unrestricted doubly occupied configuration interaction framework: a half-projection treatment

Javier Garcia[1], Diego R. Alcoba[2,3,a)], Alicia Torre[4], Luis Lain[4], Ofelia B. Oña[5], and Gustavo E. Massaccesi[6,7]

AFFILIATIONS

[1]Instituto de Física La Plata, Consejo Nacional de Investigaciones Científicas y Técnicas, and Departamento de Física, Universidad Nacional de La Plata, CC 67, 1900 La Plata, Argentina
[2]Universidad de Buenos Aires, Facultad de Ciencias Exactas y Naturales, Departamento de Física. Ciudad Universitaria, 1428 Buenos Aires, Argentina
[3]CONICET-Universidad de Buenos Aires, Instituto de Física de Buenos Aires (IFIBA). Ciudad Universitaria, 1428 Buenos Aires, Argentina
[4]Departamento de Química Física, Facultad de Ciencia y Tecnología, Universidad del País Vasco, Apdo. 644, E-48080 Bilbao, Spain
[5]Instituto de Investigaciones Fisicoquímicas Teóricas y Aplicadas, Universidad Nacional de La Plata, Consejo Nacional de Investigaciones Científicas y Técnicas, Diag. 113 y 64 (S/N), Sucursal 4, CC 16, 1900 La Plata, Argentina
[6]Departamento de Ciencias Exactas, Ciclo Básico Común, Universidad de Buenos Aires, Ciudad Universitaria, 1428 Buenos Aires, Argentina
[7]Instituto de Investigaciones Matemáticas Luis Santaló, Consejo Nacional de Investigaciones Científicas y Técnicas, Universidad de Buenos Aires, Ciudad Universitaria, 1428 Buenos Aires, Argentina

[a)]**Author to whom correspondence should be addressed:** dalcoba@df.uba.ar

ABSTRACT

The energy-variance-based optimization procedures have proven to be useful tools to describe N-electron spectra. However, the resulting wave functions usually present spin-contaminant contributions. The goal of this work is to reduce the spin contamination of the results arising from the unrestricted doubly occupied configuration interaction method in its energy variance minimization version [D.R. Alcoba *et al.*, J. Chem. Phys. **160**, 164107 (2024)]. We propose to incorporate the half projection technique, that allows to remove the spin components with even or odd spin quantum number of an approximate N-electron wave function, into the framework of the unrestricted doubly occupied configuration interaction treatment. This implementation can be carried out following several possible ways, whose results are analyzed in detail, in order to show the behavior of each procedure. Numerical determinations performed on selected strongly correlated N-electron systems, in ground and excited states, allow us to assess the most suitable procedure.

I. INTRODUCTION

For a given finite-dimensional Hilbert space, the full configuration interaction (FCI) method provides the exact electronic energies corresponding to N-electron systems. As is well known, this method expresses the N-electron wave functions by means of expansions in terms of all N-electron Slater determinants that can be constructed with the selected orbital basis set. However, the FCI method requires a high computational cost and, in practise, its use becomes prohibitive, except for small size systems [1–3]. Consequently, a great effort has been dedicated for some time now to searching for approximate methods leading to results close to the FCI ones [4–11]. The configuration interaction (CI) methods limit the number of Slater determinants used in the wave function expansions selecting them according to a determined criterion, while the remaining determinants are neglected [12, 13]. The degree of excitation of the determinants with respect to a reference and the seniority number of these determinants are the most popular selection criteria, as well as hybrid procedures combining both approaches [14–19]. In particular, the doubly occupied configuration interaction (DOCI) method [20–23] expands the wave functions over the set of determinants with zero seniority number, $\Omega = 0$, where Ω stands for the seniority number [24, 25]. The seniority number of an N-electron determinant is its number of singly occupied orbitals (or unpaired electrons), so that in the DOCI expansions all orbitals are doubly occupied. This method has been widely used, proving to be a successful procedure to describe strongly correlated systems. The results arising from the DOCI technique are basis dependent, since any unitary transformation of the basis set leads to different energy values. Hence, the use of DOCI methods requires to perform optimizations of the orbital basis sets, usually by means of energy minimization [26–28]. The orbital optimization can be accomplished in a restricted manner, in which the paired spin-orbitals have identical orbital part or, alternatively, following an unrestricted treatment where the orbital pairs can have different orbital parts. Both procedures have been denoted as RDOCI and UDOCI respectively, when the optimization is based on energy minimization [29–31]. Furthermore, the restricted and unrestricted orbital optimizations can

be performed by means of minimizations of the energy variance instead of the energy [32–35]; these methods have been denoted as σ-RDOCI and σ-UDOCI. The σ-methods avoid the variational collapse effect [36] that appears in the energy minimization approach, allowing us to determine optimal ground and excited energies within a unified treatment [37, 38].

Although the unrestricted methods in general lead to energy values closer to the FCI ones than their restricted counterpart versions, the resulting wave functions are not usually eigenfunctions of the $\hat{S}^2$ operator. This effect is a consequence of the $\hat{S}^2$ symmetry breaking inherent to the unrestricted methods and appears in the results arising from these procedures. On the other hand, the half-projection technique has proven to be a suitable tool to remove spin-contaminant contributions of the spin symmetries corresponding to states of even or odd spin quantum number S [39–45]. In this scenario, our purpose is to introduce the half-projection technique into the DOCI methodology framework, mainly with the aim of developing an efficient treatment to reduce the spin contamination of the results arising from the use of σ-UDOCI method in terms of $\langle \hat{S}^2 \rangle$ expectation values. The implementation of this procedure enables several options [46], that are described in this paper. We have applied the resulting treatments to the study of selected N-electron systems, obtaining different results in terms of energies, $\langle \hat{S}^2 \rangle$ expectation values, and wave functions. In order to carry out the corresponding assessment, these results have been compared with those arising from other approximate methods and from the FCI one.

This article has been organized as follows. In Sec. II, we report a summary of the concepts and theoretical formulations used in this work. The third section shows results obtained in several clusters of hydrogen atoms at different geometries, for which the FCI results are computationally affordable. This section also contains the computational details and the corresponding discussion. Finally, in the fourth section, we point out the main conclusions of this work.

II. THEORETICAL ASPECTS

Let us consider a non-relativistic electronic Hamiltonian $\hat{H}$, corresponding to a pairwise-interacting N-electron system with clamped nuclei. The expectation value of the dispersion operator $\hat{\sigma}^2(\omega) = (\hat{H} - \omega\hat{I})^2$ corresponding to that Hamiltonian, for an N-electron ansatz wave function Ψ, is

$$\sigma^2(\omega) = \langle\Psi|(\hat{H} - \omega\hat{I})^2|\Psi\rangle \tag{1}$$

where ω is a real parameter and $\hat{I}$ is the N-electron identity operator. If Ψ is an eigenfunction (ground or excited) of the Hamiltonian $\hat{H}$ and ω its corresponding eigenvalue, the variance $\sigma^2(\omega)$ is zero. Consequently, small values of the $\sigma^2(\omega)$ quantity indicate that the ansatz Ψ and the corresponding ω parameter value constitute suitable approximations. Within the DOCI methodology, the Ψ ansatz wave functions can be optimized by means of the energy-variance-based minimization method, for each selected ω value, providing a set of quasi-parabolas. The vertex of each parabola approximately detects the existence of an eigenstate. In this way, it is possible to describe successfully electronic spectra of N-electron systems [37, 38]. The procedure requires to perform Jacobi rotations of the spin-orbital basis set, to reach iteratively minimum values of the $\sigma^2(\omega)$ quantities. This technique can be implemented by means of orbital rotations so that the resulting spin-orbital pairs possess identical orbital part (σ-RDOCI method), or, alternatively, the rotations are performed independently for the α-orbitals and for the β-orbitals (σ-UDOCI method). To our experience, the σ-UDOCI method leads to energy numerical values and wave functions closer to the FCI ones than those provided by σ-RDOCI method, but its $\hat{S}^2$ symmetry breaking yields spin-contaminated results. As has been mentioned in the Introduction, in this work we try to restore the right spin symmetry in the results arising from the σ-UDOCI method.

A spin-contaminated N-electron wave function Ψ, resulting from the application of the σ-UDOCI method, can be expressed according to its spin components as

$$\Psi = c_S\Psi_S + c_T\Psi_T + c_Q\Psi_Q + c_H\Psi_H + \cdots \tag{2}$$

where $\Psi_S, \Psi_T, \Psi_Q, \Psi_H, \cdots$ are singlet, triplet, quintuplet, heptatuplet, $\cdots$ N-electron wave function components and $c_S, c_T, c_Q, c_H, \cdots$ their corresponding coefficients.

The half-projection technique uses the spin-conjugate N-electron wave function $\bar{\Psi}$ of the Ψ wave function

$$\bar{\Psi} = c_S\Psi_S - c_T\Psi_T + c_Q\Psi_Q - c_H\Psi_H + \cdots \tag{3}$$

in which the wave function components corresponding to odd spin quantum number (triplet, heptatuplet, etc) change their signs with respect to those of the original wave function Ψ, while the components corresponding to even spin quantum number (singlet, quintuplet, etc) maintain their signs unchanged. This feature allows to define the wave functions

$$\Psi_+ = \Psi + \bar{\Psi} = c_S\Psi_S + c_Q\Psi_Q + \cdots \tag{4}$$

and

$$\Psi_- = \Psi - \bar{\Psi} = c_T\Psi_T + c_H\Psi_H + \cdots \tag{5}$$

Obviously, according to Eqs. (3-5), the normalized Ψ_+ and Ψ_- wave functions contain less spin components than their counterpart Ψ. The mixture of singlet and triplet states is the most common situation in results arising from unrestricted methods. Consequently, the half-projection treatment turns out to be useful, since the resulting Ψ_+ wave function has no triplet (or higher-order odd spin) components and, on the contrary, the lowest spin component of the Ψ_- wave function is the triplet one, without any singlet (or higher-order even spin) components.

The combination of half-projection and σ-UDOCI techniques requires to perform two crucial steps: (i) unrestricted variational optimization of orbitals, minimizing the variance $\sigma^2(\omega)$, and (ii) half-projection to obtain wave functions with even or odd spin components. Steps (i) and (ii) correspond to the formulation of the variational-optimization and half-projection schemes, respectively. Hereafter, if step (i) is first

applied, followed by the half-projection step (ii), the resulting method will be denoted half-projection after variation σ-UDOCI (HPAV σ-UDOCI). Alternatively, if the half-projection (ii) is implemented for each iteration within step (i), the corresponding method will be called variation after half-projection σ-UDOCI (VAHP σ-UDOCI). Both procedures lead to different results and, consequently, their performances need to be assessed. In order to distinguish the situations in which the half-projections are performed on even or odd spin-quantum number states, the results arising from these methods have been denoted with the $\pm$ superscripts, HPAV$^+$ and VAHP$^+$ for even spin-quantum numbers and HPAV$^-$ and VAHP$^-$ for odd ones, in which we have dropped the tag σ-UDOCI to simplify this notation. In the next section, we report numerical results in prototype N-electron systems, that show the behavior of these treatments.

III. COMPUTATIONAL DETAILS, RESULTS, AND DISCUSSION

We have chosen strongly correlated systems, such as the H_4 clusters at different geometrical symmetries (linear, squared, and tetrahedral) and internuclear distances, to test the results arising from the HPAV$^\pm$ and VAHP$^\pm$ treatments proposed in this paper. These results have been contrasted with those obtained from the σ-UDOCI (without any type of spin projection) and FCI reference procedures. The calculations have been carried out with STO-3G atomic basis sets, in order to afford a reasonable computational cost and dispose of the exact FCI values. Those systems, described with the STO-3G basis set, present twenty singlets, fifteen triplets, and one quintuplet [6, 47]. The one- and two- electron atomic integrals and the initial molecular orbitals have been extracted from PSI4 codes [48], using the Psi4Numpy programming environment [49]. We have used our own codes to evaluate the reduced DOCI Hamiltonians [29] and the quantities related with the dispersion operator (1). The energy variance-based optimization of the orbital basis sets has been performed by means of the Broyden-Fletcher-Goldfarb-Shanno (BFGS) algorithm as is implemented in SciPy 1.0 [50].

Table I shows energies and $\langle \hat{S}^2 \rangle$ values arising from the FCI, σ-UDOCI, HPAV$^\pm$,

and VAHP$^{\pm}$ methods, for the linear H_4 cluster at 0.75Å internuclear distances (close to the equilibrium ground-state internuclear distance in the H_2 molecule). A survey of the values in Table I highlights the VAHP$^{\pm}$ treatments leading to the best results. As can be observed in that table, the VAHP$^{\pm}$ methods improve the σ-UDOCI energy results for singlets and triplets, yielding values closer to the FCI ones than their HPAV$^{\pm}$ counterparts. In the cases in which the σ-UDOCI method predicts high spin-contamination values, both VAHP$^{\pm}$ and HPAV$^{\pm}$ procedures present considerable improvements of the $\langle \hat{S}^2 \rangle$ values. In order to make a suitable comparison between the VAHP$^{\pm}$ results and those of the reference methods, we have gathered, in Fig. 1, graphical representations of the numerical values of the $\sigma^2(\omega)$ variances, arising from the VAHP$^{\pm}$ and σ-UDOCI procedures, against the ω values. That figure shows the quasi-parabolic behavior of this type of results, mentioned in the previous section. In Fig. 1, the ω values corresponding to the FCI energies have been pointed out by means of dotted vertical lines (black for singlets, red for triplets, and violet for quintuplets). We can observe in that figure that the ω values at the minima predicted by the σ-UDOCI method are close to energy values corresponding to FCI states. However, the number of σ-UDOCI quasi-parabolas is lower than that predicted by the VAHP$^{\pm}$ methods. This result can be interpreted in terms of the masking of states of different spin symmetries that has been detected in the energy-variance-based optimization procedures. This known masking effect [37, 51] is removed by means of the use of the half-projection methodology: as can be seen in Fig. 1, the VAHP^{+} method presents its minima close to the singlet FCI energy values, due to the predominant singlet character of the VAHP^{+} wave functions, and the VAHP^{-} method shows a similarly behavior with respect to the triplet spin character. Another aspect that deserves to be commented, in Fig. 1, is the magnitude of the variance values. The VAHP^{+} method yields higher $\sigma^2(\omega)$ values in its minima than the VAHP^{-} one. This fact must be interpreted in terms of singlet-quintuplet contamination that yet remains in the VAHP^{+} results, while the VAHP^{-} method produces pure triplets since a 4-electron system, such as the H_4 cluster, does not possess heptatuplet states, corresponding to spin quantum number $S = 3$. Apart from the

energies and $\langle \hat{S}^2 \rangle$ expectation values reported in Table I and visualized in Fig. 1, we have complemented this study describing the squared overlap values between the FCI wave functions and those provided by the σ-UDOCI, HPAV$^+$, HPAV$^-$, VAHP$^+$, and VAHP$^-$ methods. The values of these squared overlaps have been collected in Fig. 2, where they are indicated according to the displayed colorbar. The results arising from the VAHP$^\pm$ methods show again the best numerical values.

Results corresponding to the stretched linear H_4 cluster at 1.5Å internuclear distances are reported in Table II. Likewise, the graphical representation of the $\sigma^2(\omega)$ variance values against the ω ones and the values of the squared overlaps between wave functions for that system are shown in Figs. 3 and 4, respectively. The stretching of the linear H_4 cluster also predicts the mentioned quasi-parabolic behavior, although the obtained variances are lower than in the case of the former system (at 0.75Å internuclear distances) and, in some cases, the σ-UDOCI method produces higher spin contamination. However, the VAHP$^\pm$ procedures reduce considerably that contamination. It must be noted that the VAHP$^-$ method yields $\sigma^2(\omega) = 0$ values for the triplet states, indicating a total absence of spin contamination, in all its resolved minima (in green color within Fig. 3).

The square and tetrahedral arrangements of the H_4 clusters, at equilibrium geometrical distances, have also been studied in this work. We have collected the results of their energies and $\langle \hat{S}^2 \rangle$ values in Tables III and IV, respectively, while their squared wave-functions overlaps have been displayed in Fig. 5 and 6. Results corresponding to degenerate states are condensed into a single entry, i.e., the energy of degenerate states is only reported once in Tables III and IV, and the squared overlap is computed as the sum of the squared overlaps between the approximate wavefunction and each of the exact degenerate states. These results lead to an assessment of the reported methods similar to that described for the linear H_4 clusters and confirm the VAHP$^\pm$ as the most efficient proposed procedures.

IV. CONCLUDING REMARKS

In this work we have introduced the half-projection technique into the DOCI methodology framework. This treatment, that allows to draw out the wave function components corresponding to even or odd spin quantum number S, has been applied to lower the spin contamination that appears in the results arising from the σ-UDOCI method, which involves an energy variance optimization of the basis set. The implementation of this task can be carried out following two possible ways. One of them requires to perform the variational optimization after the half-projection (VAHP$^{\pm}$ methods). Alternatively, the half-projection can be performed once the variational optimization has been reached (HPAV$^{\pm}$ methods). These two procedures yield different results, as has been shown in this work. An analysis of our results on prototype systems shows that both treatments improve the σ-UDOCI method in terms of energy and spin contamination of the resulting wave functions, which also provide better squared overlaps with the reference FCI wave functions. Moreover, the higher improvements arise from the VAHP$^{\pm}$ methods, that are pointed out as the most suitable procedures and, consequently, their use must be recommended.

ACKNOWLEDGMENTS

The authors acknowledge the financial support from the Universidad de Buenos Aires (Grant Nos. 20020190100214BA and 20020220100069BA) and the Consejo Nacional de Investigaciones Científicas y Técnicas, Argentina (Grant Nos. PIP 11220200100467CO and PIP 11220210100821CO).

AUTHOR DECLARATIONS

Conflict of interest

The authors have no conflicts of interest.

Author Contributions

Javier Garcia: Conceptualization (equal); Software (equal); Formal analysis (equal); Investigation (equal). **Diego R. Alcoba**: Conceptualization (equal); Methodology (equal); Software (equal); Formal analysis (equal); Investigation (equal); Writing -

original draft (equal); Writing - review & editing (equal); Funding acquisition (equal). **Alicia Torre**: Conceptualization (equal); Validation (equal); Writing - original draft (equal); Writing - review & editing (equal). **Luis Lain**: Conceptualization (equal); Validation (equal); Writing - original draft (equal); Writing- review & editing (equal). **Ofelia B. Oña**: Conceptualization (equal); Methodology (equal); Software (equal); Formal analysis (equal), Investigation (equal); Funding acquisition (equal). **Gustavo E. Massaccesi**: Conceptualization (equal); Methodology (equal); Formal analysis (equal); Funding acquisition (equal).

DATA AVAILABILITY

The data that support the findings of this study are available from the corresponding author upon reasonable request.

REFERENCES

[1] I. Shavitt, B. J. Rosenberg, and S. Palakit, Int. J. Quantum Chem. **S10**, 33 (1976).

[2] I. Shavitt, Mol. Phys. **94**, 3 (1998).

[3] W. Kohn, in *Nobel Lectures in Chemistry 1996-2000* (World Scientific, Singapore, 2003).

[4] H. Nakatsuji, Phys. Rev. A **14**, 41 (1976).

[5] J. Karwowski, W. Duch, and C. Valdemoro, Phys. Rev. A **33**, 2254 (1986).

[6] L. Lain, A. Torre, J. Karwowski, and C. Valdemoro, Phys. Rev. A **38**, 2721 (1988).

[7] R. Parr, *Density-Functional Theory of Atoms and Molecules* (Oxford University Press, Clarendon Press, New York, Oxford, 1989).

[8] J. Cioslowski, *Many-Electron Densities and Reduced Density Matrices*, Mathematical and Computational Chemistry book series (Kluwer, Boston, 2000).

[9] C. Valdemoro, L. M. Tel, E. Perez-Romero, and A. Torre, J. Mol. Struct.:THEOCHEM **537**, 1 (2001).

[10] *Reduced-Density-Matrix Mechanics: With Application to Many-Electron Atoms and Molecules, Advances in Chemical Physics Vol. 134*, edited by D. A. Mazziotti (John Wiley & Sons, Inc., 2007).

[11] D. A. Mazziotti, Chem. Rev. **112**, 244 (2012).

[12] J. Buenker, S. D. Peyerimhoff, and W. Butscher, Mol. Phys. **35**, 771 (1978).

[13] C. F. Bunge, J. Chem. Phys. **125**, 014107 (2006).

[14] D. R. Alcoba, A. Torre, L. Lain, G. E. Massaccesi, and O. B. Oña, J. Chem. Phys. **139**, 084103 (2013).

[15] D. R. Alcoba, A. Torre, L. Lain, G. E. Massaccesi, and O. B. Oña, J. Chem. Phys. **140**, 234103 (2014).

[16] D. R. Alcoba, A. Torre, L. Lain, O. B. Oña, P. Capuzzi, M. Van Raemdonck, P. Bultinck, and D. Van Neck, J. Chem. Phys. **141**, 244118 (2014).

[17] D. R. Alcoba, A. Torre, L. Lain, G. E. Massaccesi, O. B. Oña, and P. Capuzzi, J. Chem.

Phys. **145**, 014109 (2016).

[18] D. R. Alcoba, A. Torre, L. Lain, O. B. Oña, G. E. Massaccesi, and P. Capuzzi, Adv. Quantum Chem. **76**, 315 (2018).

[19] F. Kossoski, Y. Damour, and P.-F. Loos, J. Phys. Chem. Lett. **13**, 4342 (2022).

[20] F. Weinhold and E. B. Wilson, J. Chem. Phys. **46**, 2752 (1967).

[21] F. Weinhold and E. B. Wilson, J. Chem. Phys. **47**, 2298 (1967).

[22] L. Bytautas, T. M. Henderson, C. A. Jiménez-Hoyos, J. K. Ellis, and G. E. Scuseria, J. Chem. Phys. **135**, 044119 (2011).

[23] P. A. Limacher, T. D. Kim, P. W. Ayers, P. A. Johnson, S. De Baerdemacker, D. Van Neck, and P. Bultinck, Mol. Phys. **112**, 853 (2014).

[24] P. Ring and P. Schuck, *The Nuclear Many-Body Problem* (Springer-Verlag, New York, 1980).

[25] D. S. Koltun and J. M. Eisenberg, *Quantum Mechanics of Many Degrees of Freedom* (Wiley, New York, 1988).

[26] M. Van Raemdonck, D. R. Alcoba, W. Poelmans, S. De Baerdemacker, A. Torre, L. Lain, G. E. Massaccesi, D. Van Neck, and P. Bultinck, J. Chem. Phys. **143**, 104106 (2015).

[27] W. Poelmans, M. Van Raemdonck, B. Verstichel, S. De Baerdemacker, A. Torre, L. Lain, G. E. Massaccesi, D. R. Alcoba, P. Bultinck, and D. Van Neck, J. Chem. Theory Comput. **11**, 4064-4076 (2015).

[28] F. Kossoski, A. Marie, A. Scemama, M. Caffarel, and P.-F. Loos, J. Chem. Theory Comput. **17**, 4756-4768 (2021).

[29] D. R. Alcoba, A. Torre, L. Lain, G. E. Massaccesi, O. B. Oña, E. M. Honoré, W. Poelmans, D. Van Neck, P. Bultinck, and S. De Baerdemacker, J. Chem. Phys. **148**, 024105 (2018).

[30] D. R. Alcoba, A. Torre, L. Lain, G. E. Massaccesi, O. B. Oña, and E. Ríos, J. Chem. Phys. **150**, 164106 (2019).

[31] J. Garcia, O. B. Oña, A. Torre, L. Lain, D. R. Alcoba, and G. E. Massaccesi, Int. J.

Quantum Chem. **123**, e27119 (2023).

[32] H.-Z. Ye, M. Welborn, N. D. Ricke, and T. Van Voorhis, J. Chem. Phys. **147**, 214104 (2017).

[33] H.-Z. Ye and T. Van Voorhis, J. Chem. Theory Comput. **15**, 2954 (2019).

[34] D. R. Alcoba, O. B. Oña, L. Lain, A. Torre, P. Capuzzi, G. E. Massaccesi, E. Ríos, A. Rubio-García, and J. Dukelsky, J. Chem. Phys. **154**, 224104 (2021).

[35] D. A. Corvalan, O. B. Oña, D. R. Alcoba, A. Torre, L. Lain, and G. E. Massaccesi, J. Chem. Phys. **157**, 204103 (2022).

[36] W. D. Allen and H. F. Schaefer, J. Chem. Phys. **87**, 7076 (1987).

[37] O. B. Oña, G. E. Massaccesi, J. I. Melo, A. Torre, L. Lain, D. R. Alcoba, and J. E. Peralta, J. Chem. Phys. **159**, 214104 (2023).

[38] D. R. Alcoba, O. B. Oña, A. Torre, L. Lain, G. Sierra, and G. E. Massaccesi, J. Chem. Phys. **160**, 164107 (2024).

[39] Y. G. Smeyers and L. Doreste-Suarez, Int. J. Quantum Chem. **7**, 687 (1973).

[40] Y. G. Smeyers and G. Delgado-Barrio, Int. J. Quantum Chem. **8**, 733 (1974).

[41] P. A. Cox and M. H. Wood, Theoret. Chim. Acta **41**, 269 (1976).

[42] P. A. Cox and M. H. Wood, Theoret. Chim. Acta **41**, 279 (1976).

[43] Z. E. Mihalka, P. R. Surjan, and A. Szabados, J. Chem. Theory Comput. **16**, 892 (2020).

[44] Z. E. Mihalka, A. Szabados, and P. Surjan, J. Chem. Phys. **154**, 234110 (2021).

[45] M. B. Ruiz, Int. J. Quantum Chem. **122**, e26889 (2022).

[46] G. E. Scuseria, C. A. Jiménez-Hoyos, T. M. Henderson, K. Samanta, J. K. Ellis, J. Chem. Phys. **135**, 124108 (2011).

[47] J. Paldus, J. Chem. Phys. **61**, 5321 (1974).

[48] D. G. A. Smith, L. A. Burns, A. C. Simmonett, R. M. Parrish, M. C. Schieber, R. Galvelis, P. Kraus, H. Kruse, R. Di Remigio, A. Alenaizan, A. M. James, S. Lehtola, J. P. Misiewicz, M. Scheurer, R. A. Shaw, J. B. Schriber, Y. Xie, Z. L. Glick, D. A. Sirianni, J. S. O'Brien, J. M. Waldrop, A. Kumar, E. G. Hohenstein, B. P. Pritchard, B. R. Brooks, H. F. Schaefer, A. Y. Sokolov, K. Patkowski, A. E. DePrince, U. Bozkaya, R.

A. King, F. A. Evangelista, J. M. Turney, T. D. Crawford, and C. D. Sherrill, "PSI4 1.4: Open-source software for high-throughput quantum chemistry", J. Chem. Phys. **152**, 184108 (2020).

[49] D. G. A. Smith, L. A. Burns, D. A. Sirianni, D. R. Nascimento, A. Kumar, A. M. James, J. B. Schriber, T. Zhang, B. Zhang, A. S. Abbott, E. J. Berquist, M. H. Lechner, L. A. Cunha, A. G. Heide, J. M. Waldrop, T. Y. Takeshita, A. Alenaizan, D. Neuhauser, R. A. King, A. C. Simmonett, J. M. Turney, H. F. Schaefer, F. A. Evangelista, A. E. DePrince, T. D. Crawford, K. Patkowski, and C. D. Sherrill, *"Psi4Numpy: An interactive quantum chemistry programming environment for reference implementations and rapid development"*, J. Chem. Theory Comput. **14**, 3504-3511 (2018).

[50] P. Virtanen, R. Gommers, T. E. Oliphant, M. Haberland, T. Reddy, D. Cournapeau, E. Burovski, P. Peterson, W. Weckesser, J. Bright, S. J. van der Walt, M. Brett, J. Wilson, K. J. Millman, N. Mayorov, A. R. J. Nelson, E. Jones, R. Kern, E. Larson, C. J. Carey, İ. Polat, Y. Feng, E. W. Moore, J. VanderPlas, D. Laxalde, J. Perktold, R. Cimrman, I. Henriksen, E. A. Quintero, C. R. Harris, A. M. Archibald, A. H. Ribeiro, F. Pedregosa, P. van Mulbregt, and SciPy 1.0 Contributors, *"SciPy 1.0: Fundamental Algorithms for Scientific Computing in Python"*, Nature Methods **17**, 261–272 (2020).

[51] G. David, T. J. P. Irons, A. E. A. Fouda, J. W. Furness, and A. M. Teale, J. Chem. Theory Comput. **17**, 5492 (2021).

TABLE I: Energies (in E_h) and spin values of the linear H_4 cluster at 0.75Å internuclear distances computed with several methods (see text). Results correspond to STO-3G atomic basis set suitably transformed for each method.

	Energy						$\langle S^2 \rangle$					
State	FCI	σ-UDOCI	HPAV$^+$	HPAV$^-$	VAHP$^+$	VAHP$^-$	FCI	σ-UDOCI	HPAV$^+$	HPAV$^-$	VAHP$^+$	VAHP$^-$
1S	-5.2026	-5.1892	-5.1892		-5.2002		0.000	0.000	0.000		0.001	
1T	-4.7998	-4.7806		-4.7806		-4.7998	2.000	2.000		2.000		2.000
2S	-4.5091	-4.5067	-4.5067		-4.5086		0.000	0.000	0.000		0.000	
2T	-4.4605					-4.4604	2.000					2.000
3S	-4.3641	-4.3287	-4.3287		-4.3614		0.000	0.000	0.000		0.005	
4S	-4.0343	-4.0926	-4.1276		-4.0277		0.000	0.462	0.007		0.018	
3T	-3.9750	-3.9145		-3.9145			2.000	2.000		2.000		
4T	-3.8052	-3.7237		-3.7879		-3.8056	2.000	0.995		2.000		2.000
5S	-3.6965				-3.6835		0.000				0.048	
6S	-3.6474		-3.5856		-3.6323		0.000		1.119		0.386	
5T	-3.5425	-3.5634		-3.5411		-3.5415	2.000	1.556		2.000		2.000
1Q	-3.4266						6.000					
7S	-3.4177						0.000					
8S	-3.3749	-3.3557	-3.3557		-3.3797		0.000	0.000	0.000		0.000	
6T	-3.2644					-3.2644	2.000					2.000
7T	-3.0041	-3.0012		-3.0012		-3.0024	2.000	2.000		2.000		2.000
9S	-3.0026						0.000					
8T	-2.9284					-2.9280	2.000					2.000
9T	-2.8601	-2.8804		-2.8817		-2.8604	2.000	1.983		2.000		2.000
10S	-2.7685		-2.7609		-2.7663		0.000		0.390		0.000	
10T	-2.7352	-2.6836		-2.6836		-2.7369	2.000	2.000		2.000		2.000
11S	-2.6481				-2.7096		0.000				0.000	
12S	-2.4774				-2.4440		0.000				0.000	
11T	-2.4555	-2.4023		-2.4990		-2.4555	2.000	1.026		2.000		2.000
13S	-2.2704	-2.2398	-2.2398		-2.3061		0.000	0.000	0.000		0.000	
12T	-2.2002					-2.1999	2.000					2.000
14S	-2.0929	-2.1019	-2.1231		-2.1222		0.000	0.845	0.001		0.001	
13T	-2.0514			-2.0723		-2.0523	2.000			2.000		2.000
15S	-2.0264				-2.0508		0.000				0.000	
16S	-1.6589	-1.6191	-1.6192		-1.6015		0.000	0.000	0.000		0.000	
17S	-1.5454						0.000					
14T	-1.5089					-1.5089	2.000					2.000
15T	-1.3037	-1.3842		-1.3861		-1.3037	2.000	2.000		2.000		2.000
18S	-1.1844				-1.0868		0.000				0.000	
19S	-0.9599	-1.0722	-1.0715		-0.9758		0.000	0.000	0.000		0.000	
20S	-0.6425	-0.6497	-0.6497		-0.6484		0.000	0.000	0.000		0.001	

TABLE II: Energies (in E_h) and spin values of the stretched linear H_4 cluster at 1.5Å internuclear distances computed with several methods (see text). Results correspond to STO-3G atomic basis set suitably transformed for each method.

	Energy						$\langle S^2 \rangle$					
State	FCI	σ-UDOCI	HPAV$^+$	HPAV$^-$	VAHP$^+$	VAHP$^-$	FCI	σ-UDOCI	HPAV$^+$	HPAV$^-$	VAHP$^+$	VAHP$^-$
1S	-3.5249	-3.4979	-3.4823		-3.5213		0.000	0.595	0.169		0.013	
1T	-3.4543	-3.4681		-3.4535		-3.4543	2.000	1.088		2.000		2.000
2T	-3.3816					-3.3816	2.000					2.000
2S	-3.3504	-3.3473	-3.3127		-3.3444		0.000	1.185	2.580		0.425	
3T	-3.3024	-3.3092		-3.3058		-3.3024	2.000	2.292		2.000		2.000
1Q	-3.2607						6.000					
4T	-2.9869					-2.9866	2.000					2.000
4S	-2.9596	-2.9392	-2.9393		-2.9362		0.000	0.000	0.000		0.001	
5S	-2.9093		-2.8693				0.000		0.004			
5T	-2.8883	-2.8664		-2.8678		-2.8883	2.000	1.041		2.000		2.000
6S	-2.8803				-2.8794		0.000				0.000	
6T	-2.8632					-2.8632	2.000					2.000
7S	-2.8446						0.000					
8S	-2.8167		-2.8644		-2.8349		0.000		0.002		0.000	
7T	-2.7847	-2.7842		-2.7842		-2.7843	2.000	2.000		2.000		2.000
8T	-2.7646					-2.7647	2.000					2.000
9T	-2.7406					-2.7406	2.000					2.000
9S	-2.6727				-2.6411		0.000				0.000	
10T	-2.6598	-2.6555		-2.6629		-2.6599	2.000	1.697		2.000		2.000
10S	-2.6106						0.000					
11T	-2.5928	-2.5844		-2.5844		-2.5926	2.000	2.000		2.000		2.000
11S	-2.5745		-2.6139				0.000		0.000			
12S	-2.5442				-2.5594		0.000				0.000	
12T	-2.5287					-2.5292	2.000					2.000
13T	-2.5276					-2.5281	2.000					2.000
13S	-2.4634	-2.4743	-2.4744		-2.4597		0.000	0.000	0.000		0.000	
14S	-2.4470						0.000					
14T	-2.3351						2.000					
15T	-2.3126	-2.3292		-2.3293		-2.3126	2.000	2.000		2.000		2.000
15S	-2.2576						0.000					
16S	-2.1705	-2.1776	-2.1778		-2.1610		0.000	0.000	0.000		0.000	
17S	-2.0984	-2.0774	-2.0779				0.000	0.000	0.000			
18S	-2.0005	-2.0155	-2.0158		-2.0105		0.000	0.000	0.000		0.000	
19S	-1.7236						0.000					
20S	-1.7231	-1.7233	-1.7233		-1.7233		0.000	0.000	0.000		0.000	

TABLE III: Energies (in E_h) and spin values of the square H_4 cluster at equilibrium internuclear distances (1.30Å) computed with several methods (see text). Results correspond to STO-3G atomic basis set suitably transformed for each method.

	Energy						$\langle S^2 \rangle$					
State	FCI	σ-UDOCI	HPAV$^+$	HPAV$^-$	VAHP$^+$	VAHP$^-$	FCI	σ-UDOCI	HPAV$^+$	HPAV$^-$	VAHP$^+$	VAHP$^-$
1S	-4.1743	-4.1507	-4.1553		-4.1518		0.000	0.835	0.086		0.021	
1T	-4.1445			-4.1436		-4.1445	2.000			2.000		2.000
2S	-4.0317	-3.9950	-4.0314		-4.0316		0.000	0.823	0.000		0.000	
2T	-3.9431			-3.9430		-3.9431	2.000			2.000		2.000
3S	-3.9021	-3.9044	-3.9039		-3.9021		0.000	0.000	0.000		0.000	
1Q	-3.7714						6.000					
3T	-3.6007					-3.6007	2.000					2.000
4S	-3.5932	-3.5291	-3.5291		-3.5918		0.000	0.000	0.000		0.000	
5S	-3.4959				-3.4803		0.000				0.000	
4T	-3.4493					-3.4493	2.000					2.000
6S	-3.4400	-3.4809	-3.4809		-3.4398		0.000	0.000	0.000		0.000	
5T	-3.3177	-3.3117		-3.3117			2.000	2.000		2.000		
6T	-3.3055	-3.3055		-3.3055		-3.3055	2.000	2.000		2.000		2.000
7S	-3.3018	-3.3018	-3.3018		-3.3018		0.000	0.000	0.000		0.000	
7T	-3.2938	-3.2938		-3.2938			2.000	2.000		2.000		
8S	-3.1957	-3.1949	-3.1960		-3.1949		0.000	0.000	0.000		0.000	
8T	-3.1944					-3.1944	2.000					2.000
9S	-3.1243				-3.1446		0.000				0.000	
9T	-3.1162	-3.0414		-3.0413		-3.1162	2.000	2.000		2.000		2.000
10S	-3.0532				-3.0527		0.000				0.000	
10T	-2.9008			-2.9010		-2.9008	2.000			2.000		2.000
11S	-2.8947	-2.9427	-2.9427		-2.8947		0.000	0.000	0.000		0.000	
12S	-2.8242	-2.8639	-2.8273		-2.8273		0.000	0.993	0.000		0.000	
11T	-2.6484					-2.6495	2.000					2.000
13S	-2.5058	-2.5109	-2.5109				0.000	0.000	0.000			
14S	-2.4876				-2.4878		0.000				0.000	
15S	-2.4303	-2.4594	-2.4594		-2.4314		0.000	0.000	0.000		0.000	
16S	-2.3669	-2.3975	-2.3974		-2.3845		0.000	0.000	0.000		0.000	

TABLE IV: Energies (in E_h) and spin values of the tetrahedral H_4 cluster at equilibrium internuclear distances (1.90Å) computed with several methods (see text). Results correspond to STO-3G atomic basis set suitably transformed for each method.

	Energy						$\langle S^2 \rangle$					
State	FCI	σ-UDOCI	HPAV$^+$	HPAV$^-$	VAHP$^+$	VAHP$^-$	FCI	σ-UDOCI	HPAV$^+$	HPAV$^-$	VAHP$^+$	VAHP$^-$
1S	-3.5454	-3.5374	-3.5452		-3.5454		0.000	0.933	0.000		0.000	
1T	-3.5286	-3.5179		-3.5286		-3.5286	2.000	2.752		2.000		2.000
1Q	-3.4802	-3.4771	-3.5058		-3.5058		6.000	3.999	3.620		3.643	
2S	-3.1333	-3.1333	-3.1333		-3.1333		0.000	0.000	0.000		0.000	
2T	-3.0971					-3.0971	2.000					2.000
3S	-3.0188	-3.0188	-3.0188		-3.0188		0.000	0.000	0.000		0.000	
3T	-2.9870					-2.9870	2.000					2.000
4S	-2.9714	-2.9714	-2.9714		-2.9714		0.000	0.000	0.000		0.000	
4T	-2.9440					-2.9440	2.000					2.000
5T	-2.9427	-2.9427				-2.9427	2.000	2.000				2.000
5S	-2.9200	-2.8919	-2.8917				0.000	0.000	0.000			
6S	-2.8138	-2.8138	-2.8105		-2.8138		0.000	0.000	0.000		0.000	
6T	-2.7751	-2.7848		-2.7785		-2.7751	2.000	1.652		2.000		2.000
7S	-2.4124	-2.4018	-2.4019		-2.4123		0.000	0.000	0.000		0.000	
8S	-2.3814	-2.3814	-2.3814		-2.3814		0.000	0.000	0.000		0.000	
9S	-2.3357	-2.3357	-2.3357		-2.3357		0.000	0.000	0.000		0.000	

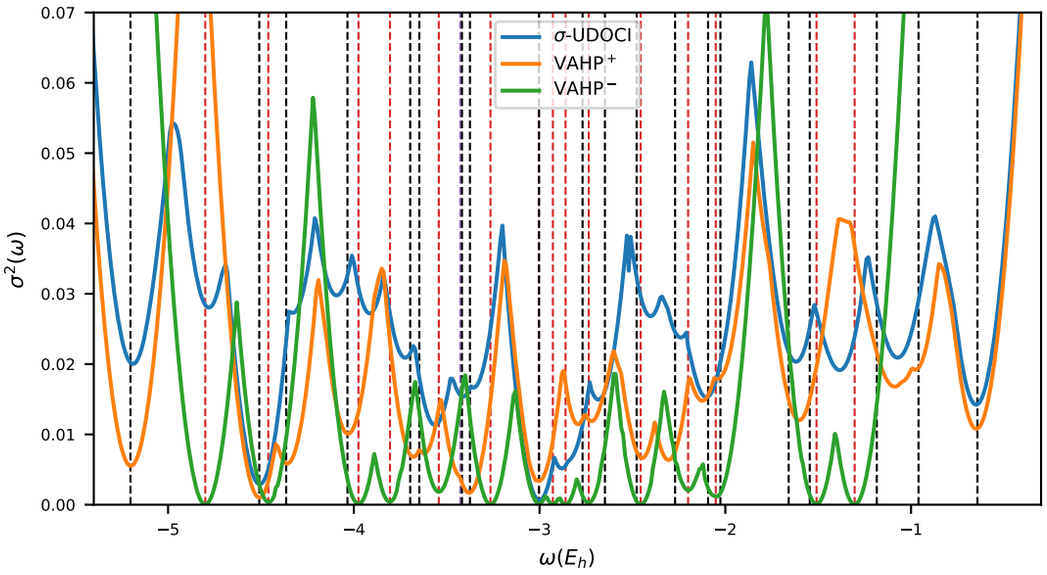

FIG. 1: Energy variances σ^2 as a function of ω, for the linear H_4 cluster at 0.75 Å internuclear distances. Results arise from the STO-3G atomic basis set transformed into the orbital set that minimizes the energy variance. FCI energies are shown in dotted lines.

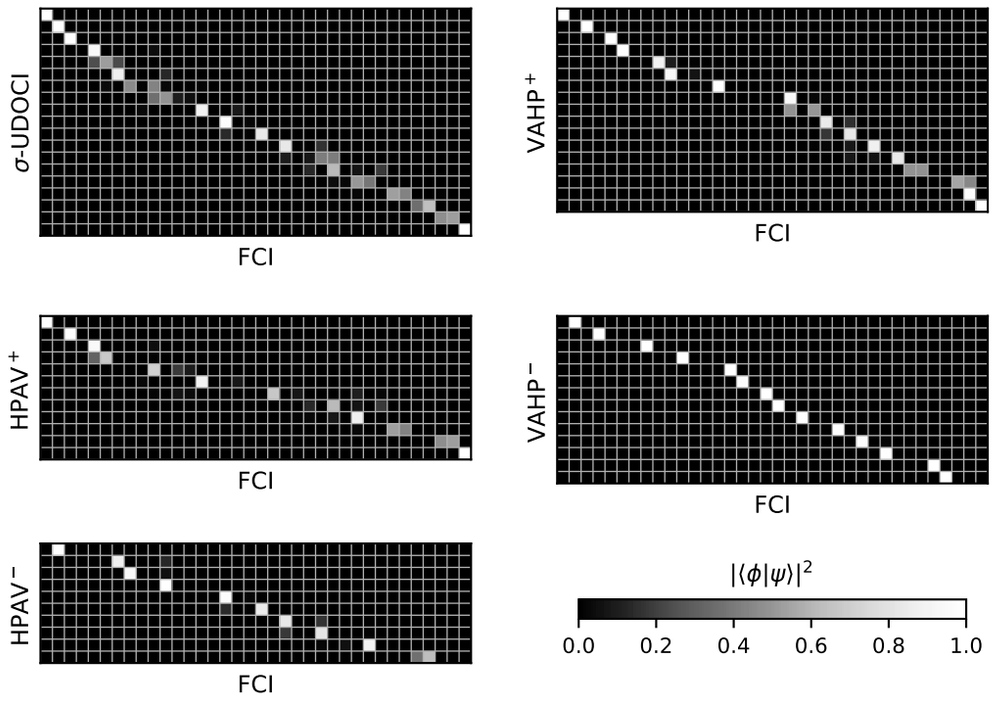

FIG. 2: Squared overlap between FCI eigenfunctions and those calculated with the σ-UDOCI, HPAV$^+$, HPAV$^-$, VAHP$^+$, and VAHP$^-$ methods for the linear H_4 cluster at 0.75Å internuclear distances. Results correspond to STO-3G atomic basis set suitably transformed for each method.

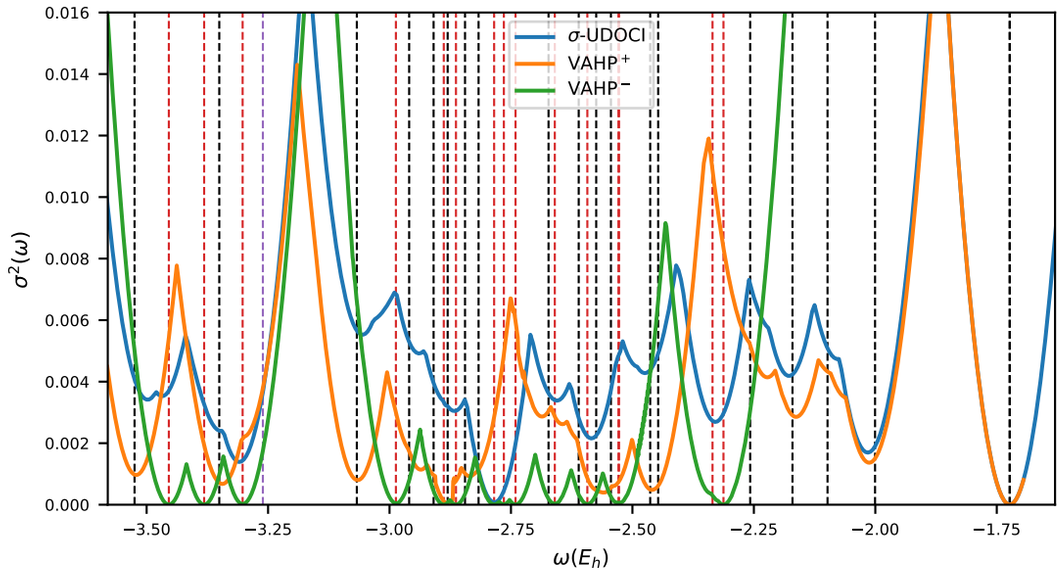

FIG. 3: Energy variances σ^2 as a function of ω, for the stretched linear H_4 cluster at 1.5 Å internuclear distances. Results arise from the STO-3G atomic basis set transformed into the orbital set that minimizes the energy variance. FCI energies are shown in dotted lines.

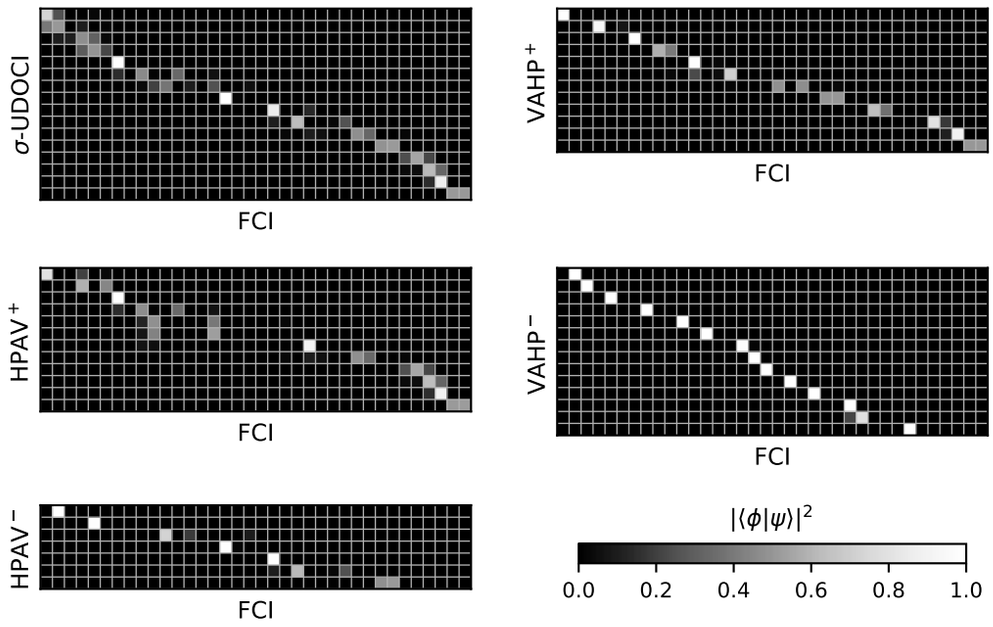

FIG. 4: Squared overlap between FCI eigenfunctions and those calculated with the σ-UDOCI, HPAV$^+$, HPAV$^-$, VAHP$^+$, and VAHP$^-$ methods for the stretched linear H_4 cluster at 1.5Å internuclear distances. Results correspond to STO-3G atomic basis set suitably transformed for each method.

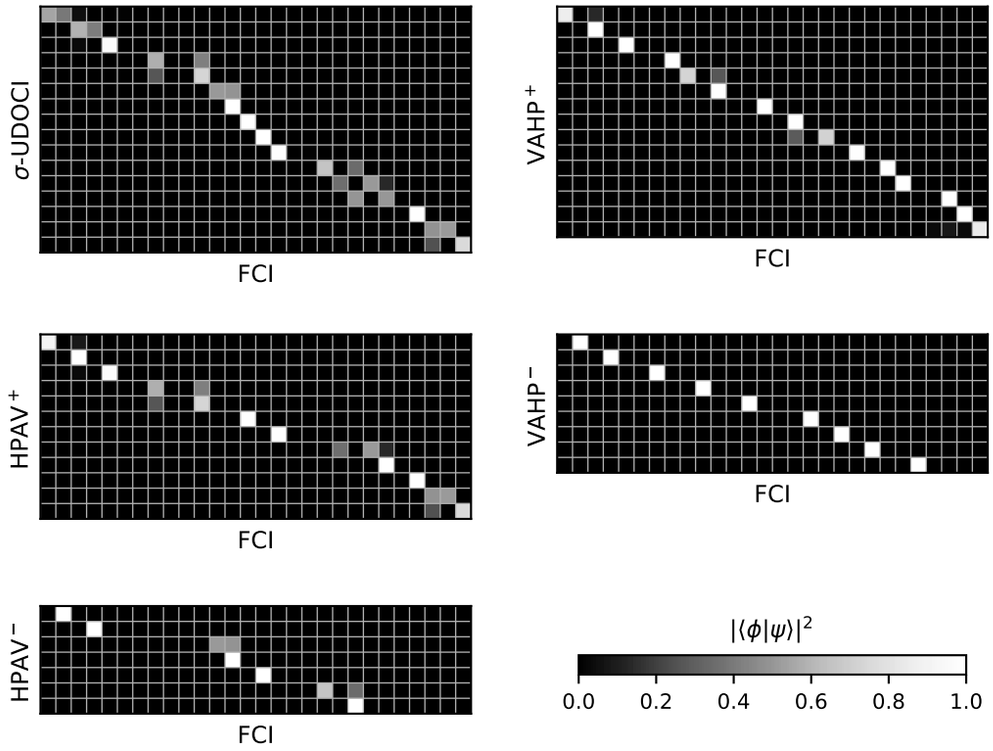

FIG. 5: Squared overlap between FCI eigenfunctions and those calculated with the σ-UDOCI, HPAV$^+$, HPAV$^-$, VAHP$^+$, and VAHP$^-$ methods for the square H_4 cluster at equilibrium internuclear distances (1.30Å). Results correspond to STO-3G atomic basis set suitably transformed for each method.

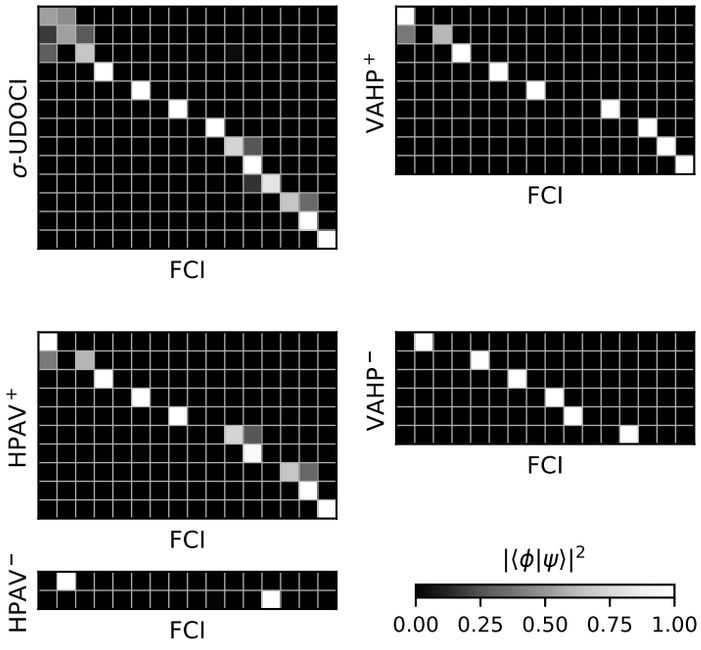

FIG. 6: Squared overlap between FCI eigenfunctions and those calculated with the σ-UDOCI, HPAV$^+$, HPAV$^-$, VAHP$^+$, and VAHP$^-$ methods for the tetrahedral H_4 cluster at equilibrium internuclear distances (1.90Å). Results correspond to STO-3G atomic basis set suitably transformed for each method.